

"This document is intended for publication in the open literature. It is made available on the understanding that it may not be further circulated and extracts may not be published prior to publication of the original, without the consent of the Publications Officer, JET Joint Undertaking, Abingdon, Oxon, OX14 3EA, UK".

"Enquiries about Copyright and reproduction should be addressed to the Publications Officer, JET Joint Undertaking, Abingdon, Oxon, OX14 3EA".

ENERGY CONFINEMENT AND H-MODE POWER THRESHOLD SCALING IN JET WITH ITER DIMENSIONLESS PARAMETERS

The JET Team¹
(Presented by J G Cordey)

JET Joint Undertaking,
Abingdon, Oxfordshire,
United Kingdom.

Abstract

An account is given of recent experiments carried out on JET to determine the scaling of the L-H and H-L power threshold and the dependence of the energy confinement on the dimensionless parameters ρ^* , ν^* and β .

1. INTRODUCTION

In JET a series of ELMy H-mode experiments has been undertaken in which the values of the dimensionless physics parameters are close to ITER values. Two physics aspects have been studied. The first, described in Section 2, is the scaling of the H-mode power threshold where, in addition to the previously reported work on the L-H transition [1] also the H-L back transition is studied. In particular, it is found that there is little hysteresis in the two threshold powers. In the second series of experiments, described in Section 3, the dependence of the confinement scaling upon the dimensionless parameters, ρ^* (larmor radius $\equiv T^{1/2}/Ba$), ν^* (collisionality $\equiv na/T^2$) and β ($\equiv nT/B^2$) is examined in turn. The dependence of energy confinement with the parameter ρ^* is obtained for a larger range of ρ^* and at higher β 's than studied previously [2],[3]. The dependence of τ_e is again found to be close to gyro-Bohm and in agreement with the ITERH93-P [4] scaling expression which is being used to predict the ITER confinement time. A similar behaviour was first found on DIII-D for low q ELMy H-modes [5]. The dependence of τ_e with ν^* , the collisionality, is also found to be in agreement with the ITERH93-P expression, whilst the scaling with β is found to be very weak in contrast to the strong scaling with β of ITERH93-P. The reasons for this discrepancy and the implications of the results of Sections 2 and 3 are discussed in Section 4.

2. H-MODE THRESHOLD SCALING STUDIES

The studies reported in reference [1] have continued in the same ITER like JET geometry $R = 2.9\text{m}$, $a = 0.92\text{m}$, $\kappa = 1.7$, $q_{\psi 95} = 3.2$, $\delta = 0.2$. The current and toroidal fields ranged from 0.83MA/0.83T to 3MA/3T. The scaling of L-H power threshold with density and toroidal field was found to be the same in the Mk IIA divertor as that of the Mk I divertor. However the range of density and field has been increased particularly at the low density end. The data obtained in Mk IIA is shown in Fig.1 versus one of the dimensionally correct forms of the threshold scaling used by F. Ryter and the ITER data base group [6]. As in Mk I there is a departure from linearity of the threshold with density at both low and high densities. However, at the low density end there is no increase in the threshold power at very low densities seen in some machines. Several different geometrical configurations have also been assessed and it has been found that there is no significant change in the threshold.

¹ See Appendix to IAEA-CN-64/O1-4, The JET Team (presented by J Jacquinot).

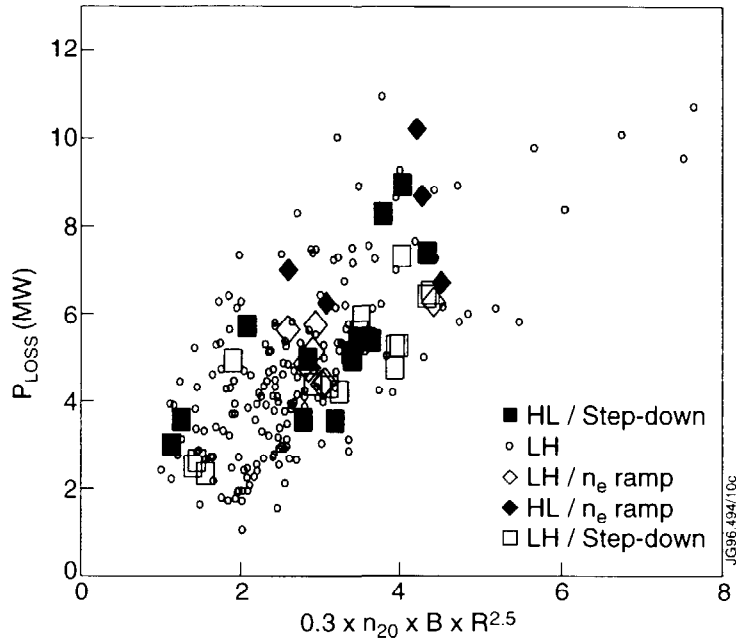


Fig.1 The loss power $P_{input} - \dot{w}$ versus $0.3 n_{20} B R^{2.5}$ ($\times 10^{20} m^{-3} T m^{2.5}$). The open symbols are for the L-H transition and the solid symbols are for the H-L transition, the rectangles are the power step down experiments, the diamonds are for the density ramp experiments, and the circles are power staircase experiments.

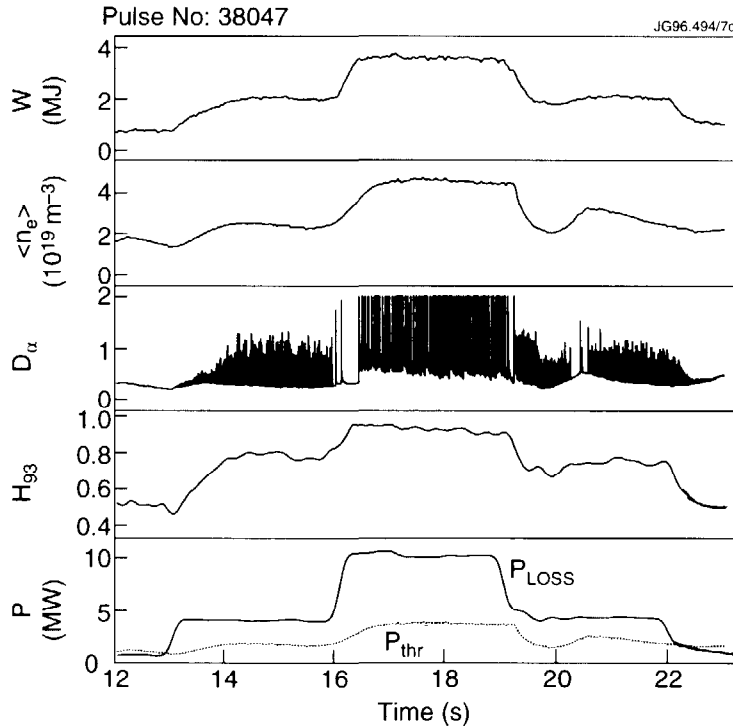


Fig. 2 Time traces of total stored energy, volume averaged density, D_{α} , H_{93} factor, and P_{loss} and the threshold power P_{thr} where the same expression as in Fig.1 was used.

Two types of experiments have been performed on the H-L back transition: (a) power step-down experiments and (b) density ramp experiments. An example of a power step-down pulse is shown in Fig.2. The NBI input power level was varied in three steps. Soon after the onset of the first 4MW step, the D_α signal indicates the presence of an H-mode by the very high frequency transition ELMs (>100 Hz). One second after the start of the heating, the stored energy and density reach steady values and the confinement enhancement factor H_{93} relative to ITERH93-P has a value ~ 0.8 . At $t=16s$ the power is further increased to 10MW, and as a result the character of the ELMs changes to the type I with a frequency ~ 20 Hz. During this period H_{93} increases to 0.95. After a steady state is achieved the power is switched down to the starting value (4MW) and the nature of the ELMs then changes back to the transition type. As a consequence, H_{93} drops to around 0.8. Finally, when the NBI power is switched off the H-mode is lost at a similar loss power to that which was required to achieve the L-H transition.

Thus there is no hysteresis in the L-H/H-L threshold in these step-down pulses. The same is found to be the case for the density ramp experiments. As the density is increased eventually the transition ELMs appear and H_{93} drops. The H-mode then disappears at a power level close to that of L-H transition for the same density. The threshold power for the H-L transition is shown in Fig.1 for both methods of obtaining a back transition along with the L-H transition data for a whole series of fields and densities from the present campaign.

3. DEPENDENCE OF τ_E ON THE DIMENSIONLESS PARAMETERS ρ^* , ν^* AND β .

Three separate groups of experiments were carried out to determine the dependence of confinement on ρ^* , ν^* and β . The plasma geometry was the same as in Section 2 and only pulses with Type I ELMs are studied in this paper. To adjust the density, only moderate gas puffing was used, the main particle source being from NBI which was the main heating source also.

The results are compared with the ITERH93-P scaling expression which can be written in dimensionless form:

$$B\tau_{th} \propto \rho^{*-2.7} \nu^{*-0.28} \beta^{-1.2} \quad (1)$$

where the parameters ρ^* , ν^* and β are defined in terms of their average values as $\rho^* \equiv W_{th}^{1/2} / n^{1/2} a^{3/2}$, $\nu^* \equiv n^3 a^7 / W_{th}^2$ and $\beta \equiv W_{th} / B^2 a^3$, with W_{th} being the total thermal stored energy, n the volume averaged density and a the minor radius.

3.1 ρ^* scaling experiments

Three sets of experiments have been completed at different β 's and collisionalities, close to those expected in ITER. These are listed in Table I. To keep ν^* and β fixed, the density should be proportional to $B^{4/3}$ and the stored energy proportional to B^2 . From Table I it can be seen that this has been approximately achieved and that the resulting dimensionless confinement $B\tau_{th}$ follows the $\rho^{*-2.7}$ scaling of ITERH93-P, that is the scaling is close to gyro-Bohm. The three ρ^* scans are shown against the scaling expression in Fig.3; H_{93} is greater than 0.9 for all of the pulses.

3.2 ν^* scaling experiments

Here β and ρ^* were kept fixed and this means that $n = \text{const.}$ and $W_{th} \propto B^2$. The results are shown in Table II. The profiles of ρ^* and β are also well matched for these two pulses as can be seen in Fig.4. From Table II it can be seen that $B\tau_{th}$ scales as $\nu^{*-0.27}$ in close agreement with the ITERH93-P scaling.

Table I ρ^* scans

a) $\beta_{nth} \sim 2$ $v^*/v^*_{ITER} = 2.8$

Pulse No.	B	I	n	P	τ_{th}	$B\tau_{th}/\rho^{*-2.7}$
37380	1	1	2.2	7	0.14	1
37375	2	2	5.6	15	0.26	1.04

b) $\beta_{nth} \sim 1.6$ $v^*/v^*_{ITER} = 1$

Pulse No.	B	I	n	P	τ_{th}	$B\tau_{th}/\rho^{*-2.7}$
38429	1.5	1.5	2.5	10	0.20	1
38427	2.6	2.6	5.0	21	0.30	0.97

c) $\beta_{nth} \sim 1.5$ $v^*/v^*_{ITER} = 2.3$

Pulse No.	B	I	n	P	τ_{th}	$B\tau_{th}/\rho^{*-2.7}$
37379	1	1	2	4.4	0.19	1
38047	2	2	4.8	10	0.34	1.03
37944	2.6	2.6	6.8	12.5	0.43	1.05

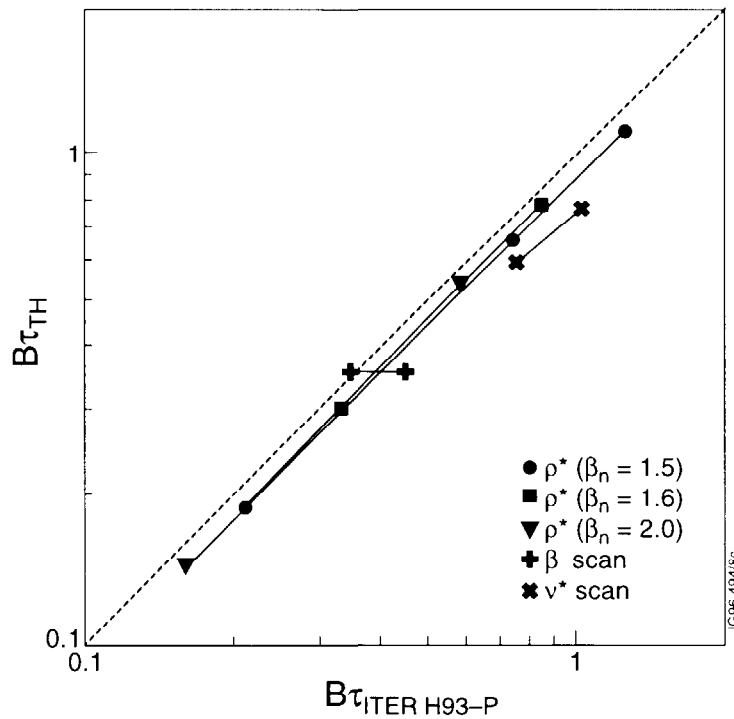


Fig.3 The normalised confinement time $B\tau_{th}$ versus $B\tau_{ITERH93-P}$. The three ρ^* scans are indicated by solid triangles, squares and circles. The β scan is indicated by the crosses and the v^* scan by the diagonal crosses.

Table II v^* and β scans

	v^* scan		β scan	
Pulse No.	37718	37728	38407	38415
B (T)	2	2.6	1.5	1.7
I (MA)	2	2.6	1.5	1.7
$\langle n \rangle$ (10^{19}m^{-3})	5	5	2.7	4.1
P (MW)	10	16	6.5	16.5
W_{th} (MJ)	3.0	4.8	1.5	3.4
τ_{th} (s)	0.3	0.3	0.24	0.21
$B\tau_{\text{th}}$	0.6	0.78	0.36	0.35
v^*/v^*_{ITER}	3.4	1.3	2.1	1.5
β_{nth}	1	1	1.2	2.2

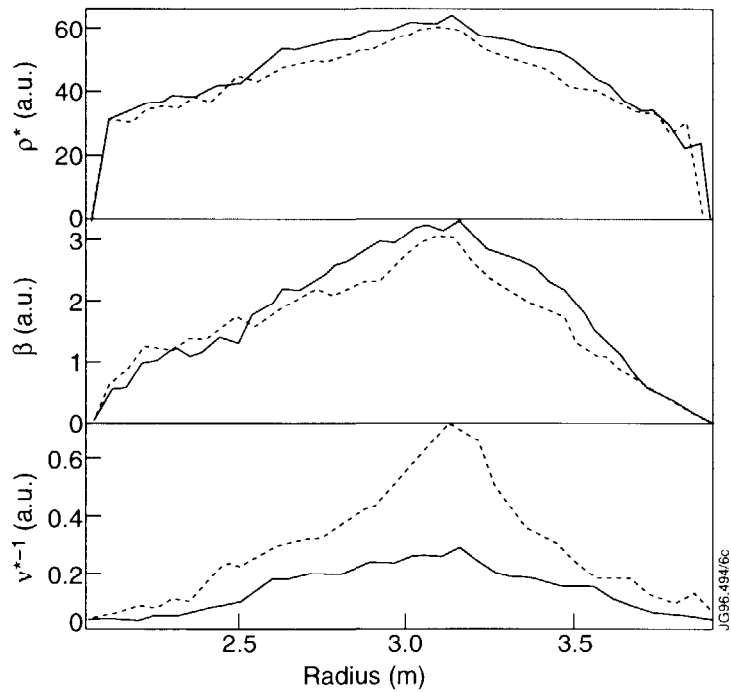


Fig. 4 Radial profiles of ρ^ , β and v^* for the pulses in the v^* scan.*

3.3 β scaling experiments

Here ρ^* and v^* were kept fixed. This means that $n \propto B^4$ and $W_{\text{th}} \propto B^6$. The results of these experiments are also given in Table II. A preliminary analysis of the data gives a very weak dependence of τ_{e} upon β with $B\tau_{\text{e}} \propto \beta^{-0.05}$, in marked contrast to the strong dependence of the ITERH93-P scaling expression. A similar result was recently found on DIII-D [7].

A comparison of both the v^* and β dependence with the ITERH93-P scaling expression is given in Fig.3. The v^* dependence follows the scaling expression whilst this is clearly not the case for the β dependence.

4. DISCUSSION

The main outcome of the threshold studies is that there are really two power thresholds. The first is the power requirement to reach steady state transition (or threshold) ELMs. There is a second power threshold for steady state periodic type I ELMs. In the transition ELM phase, the confinement improves continuously as the power is increased and the ELM frequency decreases. This phase is completely reversible and there is no hysteresis as the power is reduced. This is very similar to the situation in radiative divertors such as the CDH mode [8] where there is a smooth transition between the L and H states.

In the type I ELM phase, H_{93} reaches a higher value and is constant until the MHD β limit is reached. When the power falls significantly in the type I ELM phase, the transition ELM phase with lower confinement returns. Hence there is apparently no hysteresis in the type I ELM phase either. This latter behaviour may be different in JET to that of other devices due to the high temperature walls and high pumping which are very effective at controlling recycling in JET.

The dimensionless physics parameter scans in ρ^* , v^* and β confirm the validity of the ITERH93-P scaling expression as far as its ρ^* and v^* dependence are concerned. However, the β dependence seems not correctly described. There are several possible explanations for this discrepancy and these are currently being investigated. One obvious difference between determining the β scaling as compared with the ρ^* and v^* scaling is that the range in β is much narrower than either the ρ^* or v^* range. It is also possible that some data close to the MHD β limit has been included in the ITER data base from which ITERH93-P is derived.

If this lack of β scaling is confirmed by other experiments, the prediction of the ITER confinement time will be increased by about 10% at the β of the ignited ITER.

REFERENCES

- [1] RIGHI, E., CAMPBELL, D.J., CORDEY, J.G., et al., in Controlled Fusion and Plasma Physics (Proc. 22nd Eur. Conf. Bournemouth, 1995), Vol. 19C, Part II, European Physical Society, Geneva (1995) II-073.
- [2] BALET, B., CAMPBELL, D.J., CHRISTIANSEN, J.P., et al., *Ibid.*, Part I, I-009.
- [3] CORDEY, J.G., et al., Proceedings of the H-mode workshop PPPL (1995).
- [4] ITER H-MODE DATABASE WORKING GROUP, in Controlled Fusion and Plasma Physics (Proc. 20th Eur. Conf. Lisbon, 1993), Vol. 17C, Part I, European Physical Society, Geneva (1993) 15.
- [5] PETTY, C.C., et al., *Phys. Plasmas* **2** (1995) 2342.
- [6] RYTER, F., et al., *Nucl. Fusion* **36** (1996) 1217.
- [7] PETTY, C.C., et al., to be published in Controlled Fusion and Plasma Physics (Proc. 23rd Eur. Conf. Kiev, 1996).
- [8] KALLENBACH, A., et al., in Controlled Fusion and Plasma Physics (Proc. 22nd Eur. Conf. Bournemouth, 1995), Vol. 19C, Part II, European Physical Society, Geneva (1995) II-005.

ALFVEN EIGENMODES AND FAST PARTICLE PHYSICS IN JET REACTOR RELEVANT PLASMAS

The JET Team¹
(presented by D F H Start)

JET Joint Undertaking,
Abingdon, Oxfordshire,
United Kingdom.

Abstract

Alfven eigenmodes have been directly excited by using the JET saddle coils with a system which locks the drive frequency to the mode frequency. The technique has shown that neutral beams do not excite low n modes whereas high n modes are destabilised. Such modes are often generated by NBI alone in hot ion H-mode plasmas when the Alfven speed is about three times the parallel velocity of the beam ions. Kinetic TAE modes have been identified and theoretical calculations predict that these should be destabilised at the fast ion densities present. A new technique for generating TAE modes with ICRH beat waves has been demonstrated. Simulated α -particle heating by ICRH accelerated fast ions has produced electron temperatures of 15keV in hot ion H-modes and in shear reversed plasmas. Third harmonic ICRH has achieved a D-D neutron rate of $9 \times 10^{15} \text{s}^{-1}$ which is well simulated by PION code calculations.

1. INTRODUCTION

In a tokamak reactor the slowing down of α -particles will provide the main source of plasma heating. From present day experiments there is evidence that the slowing down is classical. Two important consequences are discussed in this paper. Firstly, the α -particle population is characterised by energies greater than the equipartition energy so that the energy is transferred to the electrons in the core region. A burning plasma will have T_e close to, but higher than T_i . Such plasmas with $T_e = 15 \text{keV}$ and $T_i = 14 \text{keV}$ have been achieved in JET with fast particle heating. These values approach the expected temperatures at ignition on ITER ($\approx 20 \text{keV}$), although at lower density. Thus the JET discharges allow electron and ion heat transport to be studied at temperatures relevant to the ignition path and the burn phase in a reactor. Transport analysis results are given for these plasmas and for reversed shear discharges in which T_e and T_i reached 15keV and 32keV, respectively. Secondly, the α -particles generate pressure gradients that can drive collective instabilities such as Alfven eigenmodes. Extensive studies of these modes have been made on JET by both direct and indirect excitation methods.

2. FAST PARTICLE PHYSICS

ICRF heating at the deuterium third harmonic resonance has provided the most stringent test of both fast particle confinement in JET and the accuracy of

¹ See Appendix to IAEA-CN-64/O1-4, The JET Team (presented by J Jacquinot), together with R Heeter, Princeton Plasma Physics Laboratory, Princeton, USA, P Lavanchi, J Lister and Y Martin, CRPP, Lausanne, Switzerland, L C Appel and S Pinches, UKAEA, Culham Laboratory, Abingdon, UK, F Nguyen, CEA, Cadarache, France, and J Candy, Institute for Fusion Studies, University of Texas, Texas, USA.

simulation codes such as the PION code [1]. The results of these experiments are given in section 2.1. Minority ICRH provides a good simulation of α -particle heating in ITER since the minority ions might reach MeV energies and fast ion beta can exceed that of the α -particle population in a reactor. Collisional transfer of the fast ion energy takes place to the electrons and this feature is exploited to investigate electron heat transport in a variety of plasma regimes. Such measurements complement ion transport studies with neutral beams which typically transfer 80% of their energy to the majority ions. The results of electron heating experiments, which achieved central temperatures up to 15keV, are described in section 2.2.

2.1 Third harmonic ICRH.

These experiments were carried out with the third harmonic deuterium resonance in the centre of a 2MA plasma with a toroidal field of 2.2T. Transit time magnetic pumping (TTMP) was the main competing damping mechanism to the cyclotron damping. The time evolution of the neutron rate (Fig.1) increases strongly during the high power RF phase and reaches $9 \times 10^{15} \text{s}^{-1}$ which is a record

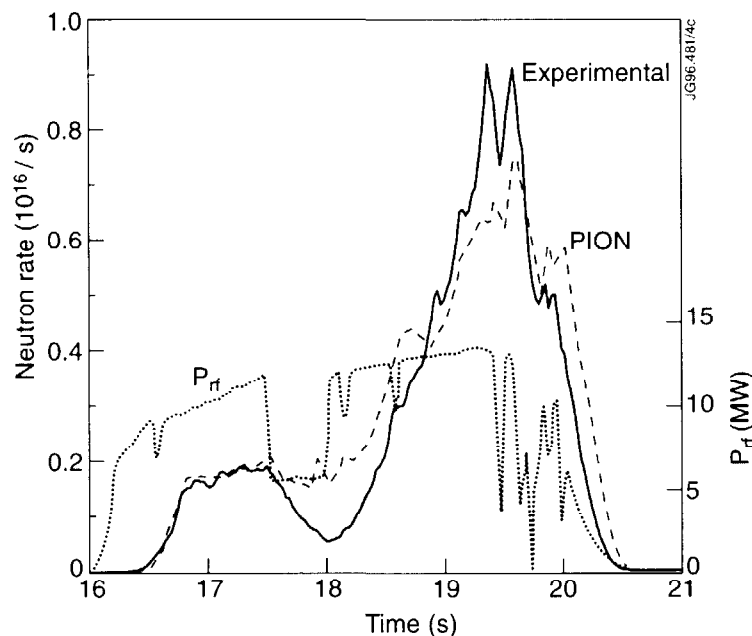


Fig.1 Experimental and PION code neutron rate for $3\omega_{CD}$ ICRH

for ICRH in JET. The neutron rate is the same as that achieved with NBI at the same power level in a similar discharge and is produced by the energetic deuterium tail. A simulation of the time evolution of the D-D neutron rate (Y_{DD}) has been made with the PION code which produces a self-consistent calculation of the power absorption and the deuterium tail. It includes TTMP absorption and effects due to the finite orbit of the fast tail. The result is shown in Fig.1. To achieve the good agreement with experiment it was necessary to include a "parasitic damping" of the order of 4% per pass and a particle loss term that removed particles with energy in excess of 4MeV which were not confined in the plasma. The parasitic damping only played a role at the beginning of the RF pulse when the tail energy was low, and was essential to obtain the time delay between the start of the RF pulse and the rise of Y_{DD} . A similar level of parasitic damping is found in TTMP current drive experiments in DIII-D and could be due to wall loss, RF sheath formation or hydrogen minority damping at the

plasma edge. The strong increase in Y_{DD} at the end of the pulse is due to the density increase which reduces the tail energy and also the number of lost ions so that the fast particle density remains almost constant. Thus the D-D neutron rate due to the interaction between the fast tail and thermal ions increases in proportion to the deuterium density.

2.2 Electron heating and transport.

These experiments have been carried out in hot ion H-modes, central reversed shear discharges and RF-only H-modes. The plasma currents ranged from 2.5MA to 3.5MA and the toroidal fields from 2.6T to 3.4T. The RF frequency was chosen to locate the hydrogen minority resonance layer in the plasma centre. The highest central value of $T_e = 15\text{keV}$ was produced in a 3MA/3.1T reversed shear plasma with 14MW of NBI and 5MW of ICRH, but similar temperatures were also achieved in the hot ion H-modes and RF-only H-modes in high triangularity plasmas.

Transport analyses of several of the discharges have been made with the TRANSP code. The results are characterised by the values of χ_e at a minor radius $r/a = 0.3$. The highest performance discharges have very similar values of χ_e ($r/a = 0.3$) close to $0.5\text{m}^2/\text{s}$. The 3MA RF-only H-modes have χ_e ($r/a = 0.3$) $\approx 1\text{m}^2/\text{s}$. For the hot ion H-modes the value of χ_i is about 50% greater than χ_e whereas χ_i is generally less than χ_e inside the confinement barrier of reversed shear plasmas.

3. ALFVEN EIGENMODES

Over the α -particle slowing down time, the fast ion cross field transport, associated with both neo-classical and anomalous effects due to electrostatic or electromagnetic turbulence, is in general negligible. Significant transport and losses of suprathreshold particles may take place only in the presence of waves which resonate with them. Of particular importance are weakly damped modes with phase velocities of the order of the α -particle speeds before thermalisation, such as Alfvén eigenmodes (AE) which exist within the gaps of the shear Alfvén spectrum in magnetically confined toroidal plasmas. It is estimated that if the α -particle losses in ITER are greater than 2% they might damage the first wall and if greater than 20% the fusion reaction will be quenched. Furthermore, Alfvén eigenmodes will resonate with the 1MeV neutral beams planned for ITER and might reduce current drive capability. The following sections present studies of the stability of Alfvén eigenmodes, excitation by fast particles and ICRF beat waves and the effect on fast ions.

3.1 Stability studies with direct excitation.

The saddle coils in JET are used to excite low n Alfvén eigenmodes in the 30kHz to 500kHz range and the modes are detected with a set of toroidal and poloidal synchronous detector coils plus ECE and reflectometer diagnostics. The Alfvén character of the modes has been verified by the scaling of the resonant frequency with density and magnetic field [2]. Recently, a system has been installed to lock the drive frequency to that of a single mode and to track this mode in real time. An example is shown in Fig.2 where a mode is detected at 7.3s close to the expected TAE frequency and is tracked until 10.5s. A small sweep is imposed on the resonance frequency to enable the damping to be measured as a function of time. In this case the damping rate (γ) is consistent with radiative damping. The locking gives a powerful technique for studying fast particle effects on mode stability. In a discharge heated by 3MW of 140keV NBI the width of the resonance ($\gamma/\omega \approx 1\%$) of a driven $n = 1$ mode increased by a factor of two compared with the value in the ohmic phase. Since $\gamma = \gamma_{\text{damping}} - \gamma_{\text{drive}}$, it appears that the fast ions produce extra damping and do not drive low n modes.

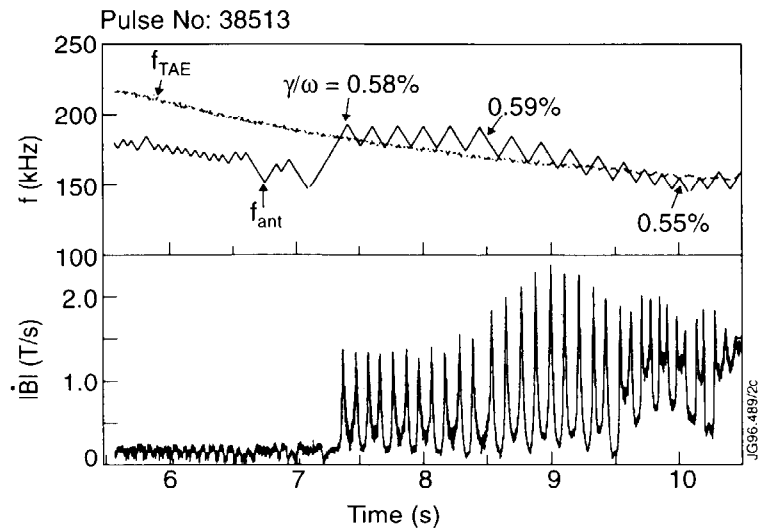


Fig.2 TAE excitation with mode-locked saddle coil drive frequency

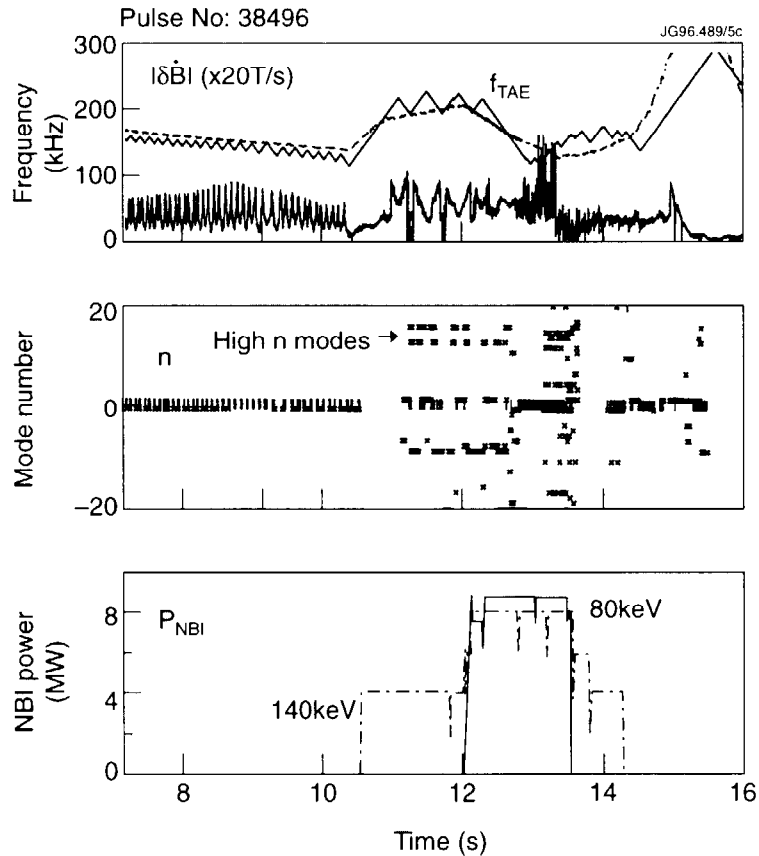


Fig.3 High n TAE modes driven unstable by 140keV NBI

This conclusion is supported by the observations shown in Fig.3. During the ohmic limiter phase the system locks to an $n = 1$ mode driven by the saddle coils. Then a divertor plasma is formed and the NBI is applied at 10.5s. At this point the driving term is dominated by the fast ions, the mode locking ceases but the system still applies the calculated TAE frequency as reference for the detection

coils. During the NBI phase high n modes are seen and these have similar amplitudes at the edge to the $n = 1$ mode in the limiter phase ($\delta B/B \approx 10^{-6}$). In the core region the amplitude of the high n modes can be several hundred times greater (for kinetic TAE modes) than the amplitude at the edge; for the $n = 1$ modes the maximum amplitude is similar to the edge magnetic field. Thus $\delta B/B$ could be higher than 10^{-4} which is approaching the threshold (10^{-3}) for stochasticity and reduced fast ion confinement. The excitation of high n modes by 140keV beams with $v_{||} = v_A/3$, where v_A is the Alfvén speed, agrees with calculations using the CASTOR code [3] which predict, for example, an $n = 14$ kinetic TAE (KTAE) to be excited at $\beta_{fast} \geq 1\%$: in Fig.3 the value of β_{fast} was 1.3%.

3.2 Excitation by fast particles.

In JET hot ion H-modes there is invariably Alfvén eigenmode excitation when $v_{||}$ of the 140keV beams is close to $v_A/3$. An example is shown in Fig.4. The TAE system was in detection mode (no saddle coil excitation) in which the reference frequency is derived from the calculated Alfvén frequency plus a small modulation. The Alfvén frequency decreases during beam heating since the density is increased due to both the NBI fuelling and the formation of an ELM-free H-mode at 12.1s. As $v_{||}$ approaches $v_A/3$ there is a strong increase in the Alfvén mode activity. There is also a tendency for the neutron rate to saturate and even decrease (roll-over). Such a degradation is often associated with either a sawtooth crash or a giant ELM but this is not the case for the discharge shown in

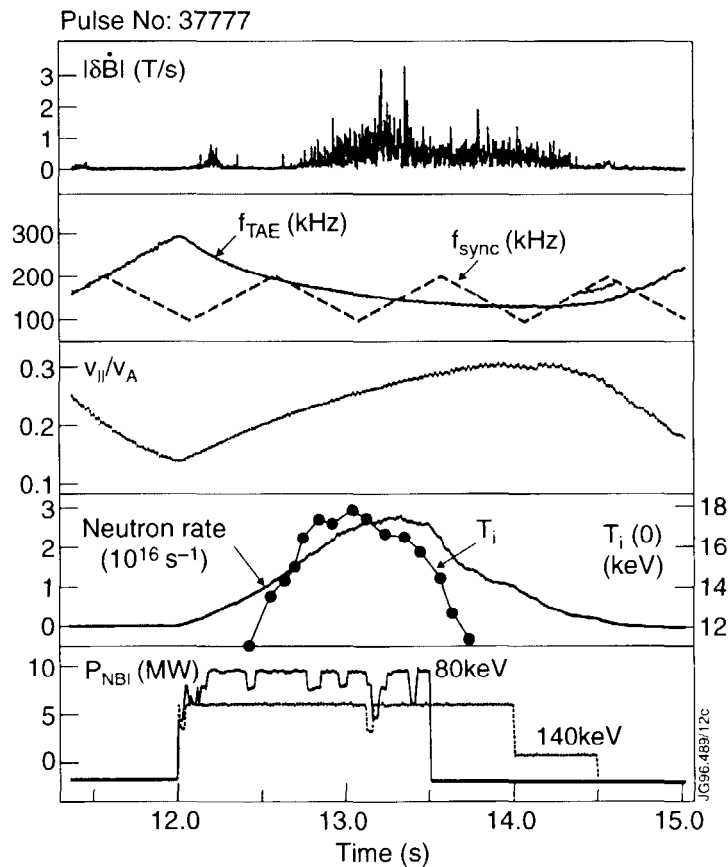


Fig.4 TAE modes excited by NBI at $v_{||} \approx v_A/3$ in a hot ion H-mode.

Fig.4. Some statistics of the resonance condition at the soft roll-over for the 140keV beams are shown in Fig.5. These data were taken for plasma currents ranging from 1.7MA to 5.1MA and for toroidal fields between 2.1T and 3.4T. Almost all the points lie in the range $v_{||}/v_A = 0.3 \pm 0.05$.

Since the signals are of the order of 10^{-6} T the eigenmodes need to be kinetic TAE to possibly affect fast ion confinement. Such KTAE modes [3] have been driven by the saddle coils. An example is shown in Fig.6 for a 3MA, 3.1T plasma heated by 6MW of ICRH and 2.5MW of lower hybrid heating. Figure 6 shows the magnetic field and density oscillation amplitudes. The constant frequency difference between modes for the same mode number and the fact that the frequencies are greater than the TAE frequency are characteristic of KTAE modes.

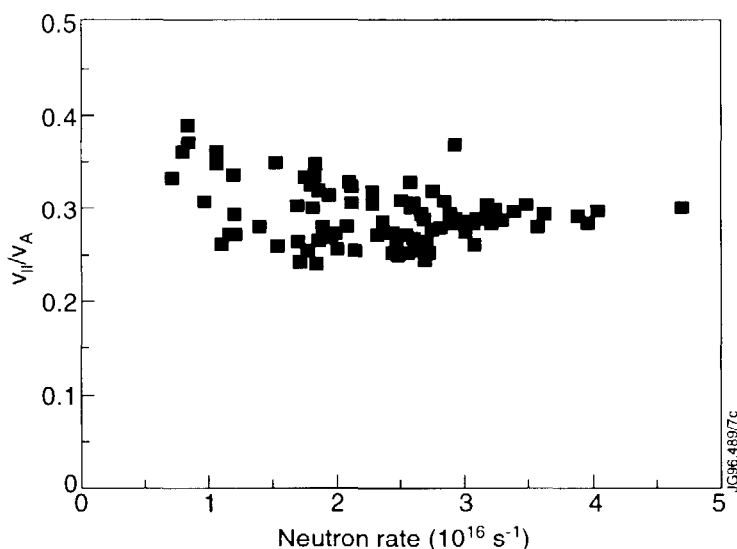


Fig.5 Ratio of $v_{||}/v_A$ for TAE destabilisation in hot ion H-modes

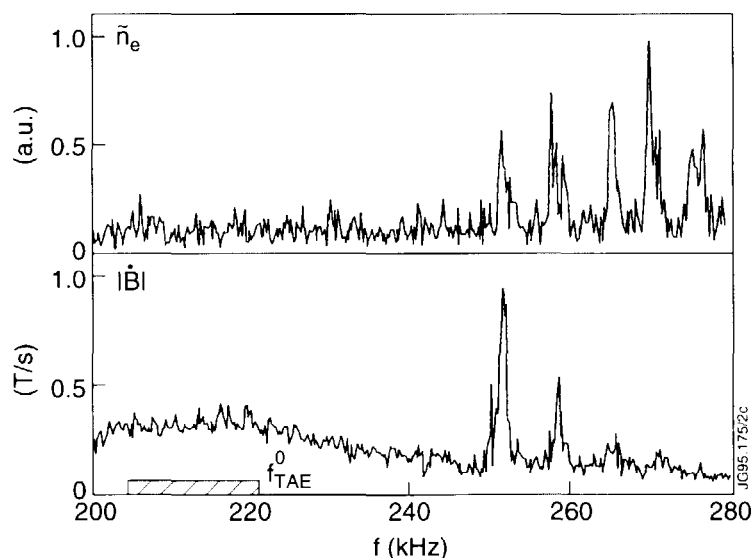


Fig.6 Observation of KTAE modes in an ICRH + LHCD heated plasma

Theoretical calculations of the effect of KTAE modes on the fast ion distribution have been made using the HAGIS code [4] which gives a self-consistent treatment of the wave field and the fast ion distribution. HAGIS is an efficient Monte Carlo code which treats just the perturbation of the fast ions thereby saving a factor of 10^2 in the number of particles required. An example is shown in Fig.7 for α -particles with $\langle\beta\rangle\sim 10^{-3}$, which is similar to values expected for 10MW of D-T fusion power in JET. The $n=6$ mode rises with a $\gamma/\omega = 3\%$ to a saturated level $\delta B/B=10^{-3}$. Such a value is close to the threshold for stochasticity.

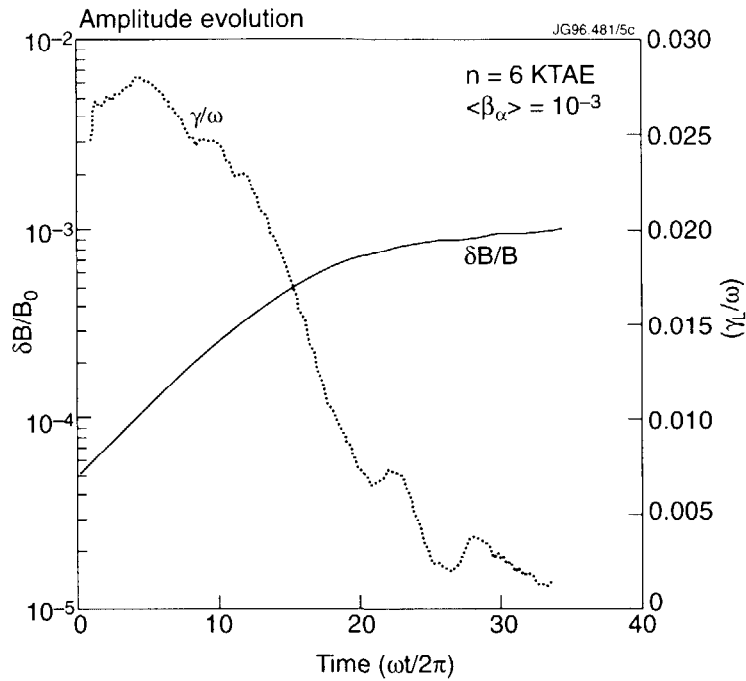


Fig.7 HAGIS prediction of KTAE amplitude and growth rate for 0.1% β_{fast}

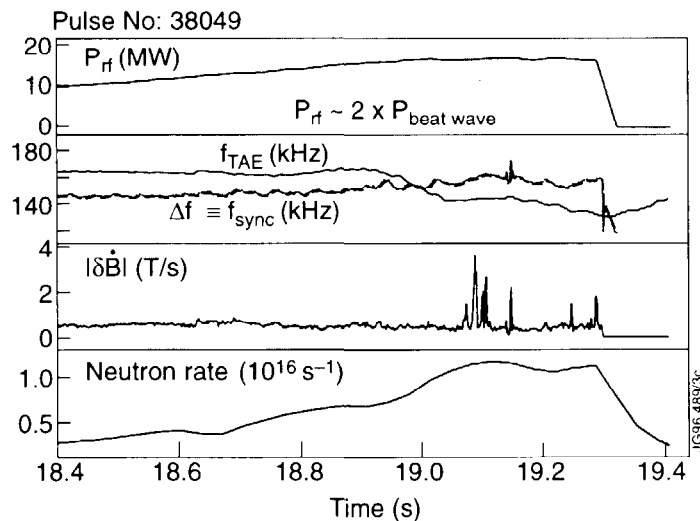


Fig.8 ICRH beat wave drive of TAE modes.

3.3 Excitation by ICRH beat waves.

Figure 8 shows the excitation of $n = 3$ TAE modes using ICRH beat waves [5]. In this discharge the difference in frequency between two ICRH antennas is around 160kHz and when the TAE frequency is close to this value (140kHz), TAE modes occur with large amplitude. Optimisation experiments have shown that the largest amplitude TAE modes are produced when the antenna phasing is 0π and adjacent rather than opposite antennas are used, probably due to the greater overlap of the RF fields.

4. SUMMARY

The JET saddle coils have been used to excite low- n TAE modes with a system which locks to the resonance frequency. The technique has demonstrated that fast neutral beam ions do not excite low n modes but can drive high n -modes unstable in accordance with theoretical expectations. The system will also be used in JET D-T experiments to measure the intrinsic excitation by α -particles. Neutral beam ions produce TAE modes when $v_{//} = v_A/3$ and there is possible evidence of performance limitation by such activity. Kinetic TAE modes have been observed and theoretical calculations suggest that these can be driven unstable at a fast ion beta value of only a few percent. A new method of directly exciting TAE modes using beat waves generated by fast waves has been established. Simulated α -particle heating using MeV fast ions generated by ICRH has produced electron temperatures up to 15keV. Transport analysis of such discharges has shown a factor of two improvement in χ_e in the core of hot-ion H-modes and reversed shear plasmas compared to RF-only ELMy plasmas. A neutron rate of $9 \times 10^{15} \text{s}^{-1}$ has been attained by third harmonic deuterium ICRH. This has been successfully reproduced by the PION code which is used extensively to predict D-T performance in JET and ITER.

ACKNOWLEDGEMENT

This work was performed under Task Agreements with CRPP, Lausanne, Switzerland, UKAEA Culham Laboratory, Abingdon, UK and CEA, Cadarache, France, and in collaboration with Princeton Plasma Physics Laboratory, Princeton, USA and Institute for Fusion Studies, University of Texas, Texas, USA.

REFERENCES

- [1] ERIKSSON, L.G., et al., Nucl. Fusion **33** (1993) 1037.
- [2] FASOLI, A., et al., Nucl. Fusion **35** (1995) 1485.
- [3] HUYSMANS, G.T.A., et al., Phys. Fluids **B 5** (1993) 1545.
- [4] APPEL, L.C., et al., Nucl. Fusion **35** (1995) 697.
- [5] FASOLI, A., et al., Nucl. Fusion **36** (1996) 258.